


 Cite this: *RSC Adv.*, 2025, **15**, 13753

## Brønsted acidic surfactant $[\text{HDMM}]^+$ $[\text{HSO}_4]^-$ : a green microreactor assembly for stereoselective synthesis of novel thiazolyl-pyrazole-chromen-2-ones in water<sup>†</sup>

Mayuri V. Patil,<sup>a</sup> Pradeep M. Mhaldar,<sup>b</sup> Vrushali M. Mahadik,<sup>a</sup> Rinku Ghanta,<sup>c</sup> Madhulata Shukla,<sup>d</sup> Suraj A. Sonawane,<sup>e</sup> Suresh K. Ghotekar,<sup>f</sup> Gajanan S. Rashinkar<sup>a</sup> and Dattaprasad M. Pore<sup>a</sup>                                       <img alt="ORCID iD icon" data-bbox="845 7155 860

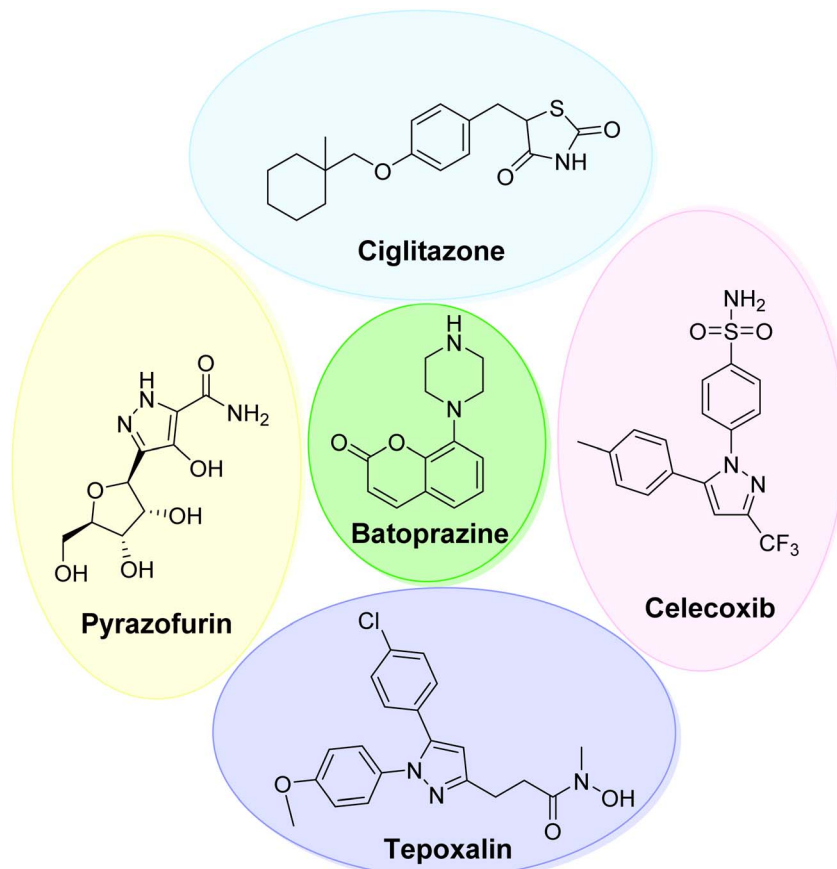
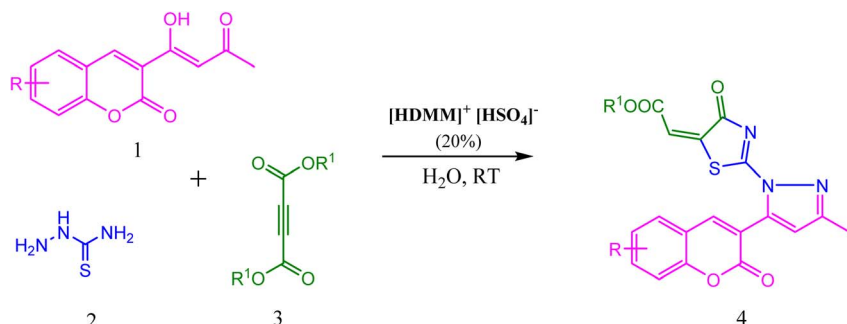


Fig. 1 Representative examples of bioactive compounds containing coumarin, pyrazole and thiazolidinone scaffolds.

Open Access Article. Published on 28 April 2025. Downloaded on 1/22/2026 12:15:12 PM.  
This article is licensed under a Creative Commons Attribution 3.0 Unported Licence.  

 chemistry and exhibit a range of biological activities.<sup>33–35</sup> Anisoucoumaramide and clauhainanin-A isolated from *Clausena anisum-olens* and *Clausena hainanensis* exhibit remarkable pharmacological properties.<sup>36,37</sup> Coumarin derivatives obtained from natural sources include dicoumarol, warfarin, acenocoumarol, and coumachlor. They are widely used to decrease blood coagulation.<sup>38</sup> In addition, various molecules containing a coumarin skeleton have applications as photosensitizers,<sup>39</sup> fluorescent chemosensors<sup>40</sup> for light energy harvesting,<sup>41</sup> and electroluminescent materials<sup>42</sup> and in soaps, perfumes, and detergents.<sup>43</sup>

Considering the importance of thiazolidine-4-one, pyrazole, and coumarin derivatives, and as a part of our endeavour towards the synthesis of a new class of biologically potent heterocyclic hybrids using a green chemistry protocol, herein, we report a highly efficient method for the diversity-oriented synthesis of thiazolyl-pyrazole-chromen-2-ones *via* a one-pot reaction of acetoacetyl coumarin, thiosemicarbazide, and dialkyl acetylene dicarboxylate in the presence of hexadecyl methyl morpholinium hydrogen sulphate ( $[\text{HDMM}]^+ [\text{HSO}_4]^-$ ) as an efficient and reusable Brønsted acidic surfactant catalyst (Scheme 1).



Scheme 1 Synthesis of thiazolyl-pyrazole-chromen-2-ones.

## 2 Results and discussion

The catalyst significantly affects various factors in organic synthesis; hence, it is a key parameter. The scientific community is continuously making efforts to develop organic transformations in aqueous medium using a benign catalytic system and avoiding toxic catalysts. Hence, initial attention was focused on the design and synthesis of a novel catalyst, *viz* Brønsted acidic surfactant (Fig. 2).

The synthesis of 4-hexadecyl-4-methylmorpholin-4-ium hydrogen sulphate,  $[\text{HDMM}]^+ [\text{HSO}_4]^-$ , is depicted in Scheme 2. The quaternization of 4-methylmorpholine with 1-bromo hexadecane in acetone is carried out by refluxing the reaction mixture at  $60^\circ\text{C}$  for 24 h to afford 4-hexadecyl-4-methylmorpholin-4-ium bromide,  $[\text{HDMM}]^+ [\text{Br}]^-$ , followed by anion exchange with conc.  $\text{H}_2\text{SO}_4$  in dry toluene at  $80^\circ\text{C}$  for 24 h furnished 4-hexadecyl-4-methylmorpholin-4-ium hydrogen sulphate,  $[\text{HDMM}]^+ [\text{HSO}_4]^-$ , a Brønsted acidic surfactant. The absence of bromide ions was examined by testing the reaction

of the surfactant with  $\text{AgNO}_3$ . The synthesized catalyst was confirmed by FTIR,  $^1\text{H}$ ,  $^{13}\text{C}$  NMR, CMC, and TGA analyses. The obtained spectroscopic data fully agreed with the structure of the surfactant catalyst.

The critical micelle concentration (CMC) of a surfactant solution was determined by applying the conductometric method. Fig. 3 illustrates the plot of CMC with coordinates equivalent conductance ( $k$ ) *versus* surfactant concentration. The CMC of  $[\text{HDMM}]^+ [\text{HSO}_4]^-$  was found to be  $0.0037 \text{ mol dm}^{-3}$ .

The thermo gravimetric analysis (TGA) was performed at temperature ranging from  $25$  to  $1000^\circ\text{C}$  under aerobic conditions at  $10^\circ\text{C min}^{-1}$  (Fig. 4). Initially, a weight loss of  $4.515\%$  was observed in the temperature range of  $25$ – $200^\circ\text{C}$  owing to the loss of physically adsorbed water from the catalyst. Further, the large weight loss of  $75.61\%$  in the range of  $200$ – $330^\circ\text{C}$  is attributed to the exothermic decomposition of the organic moiety. The third weight loss of  $18.81\%$  is due to the decomposition of residual carbonaceous species.

### 2.1 Small-angle X-ray scattering (SAXS) analysis

To elucidate the micelle diameter and the intermicellar spacing of  $[\text{HDMM}]^+ [\text{HSO}_4]^-$ , small-angle X-ray scattering (SAXS) analysis was performed. SAXS data for the samples were obtained using a Xenocs SA-France instrument, employing  $\text{CuK}\alpha$  X-rays with a wavelength of  $1.54 \text{ \AA}$ . The sample was placed in a quartz capillary, and measurements were collected for ten

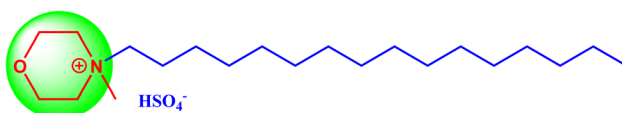
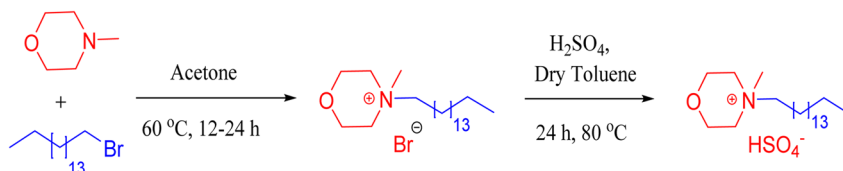


Fig. 2 Brønsted acid surfactant catalyst,  $[\text{HDMM}]^+ [\text{HSO}_4]^-$ .



Scheme 2 Synthesis of a novel Brønsted acidic surfactant,  $[\text{HDMM}]^+ [\text{HSO}_4]^-$ .

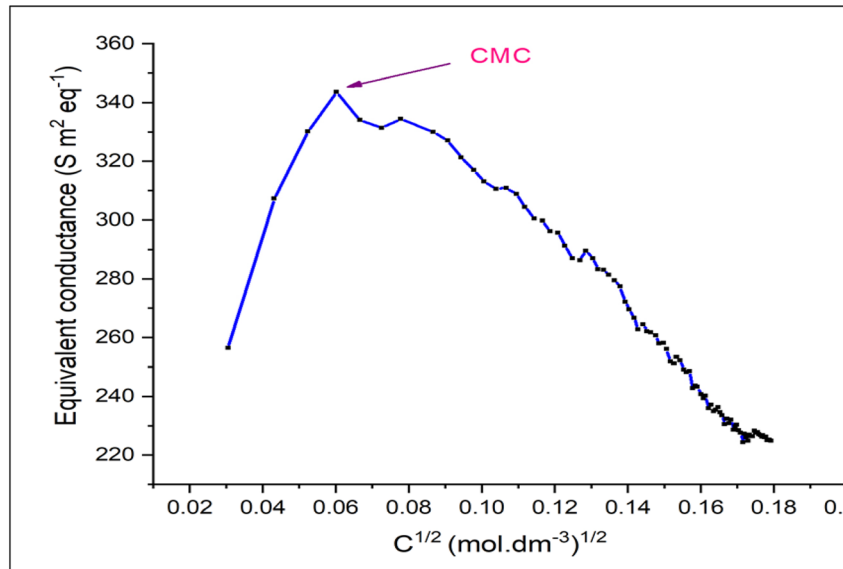


Fig. 3 Equivalent conductance as a function of concentration.



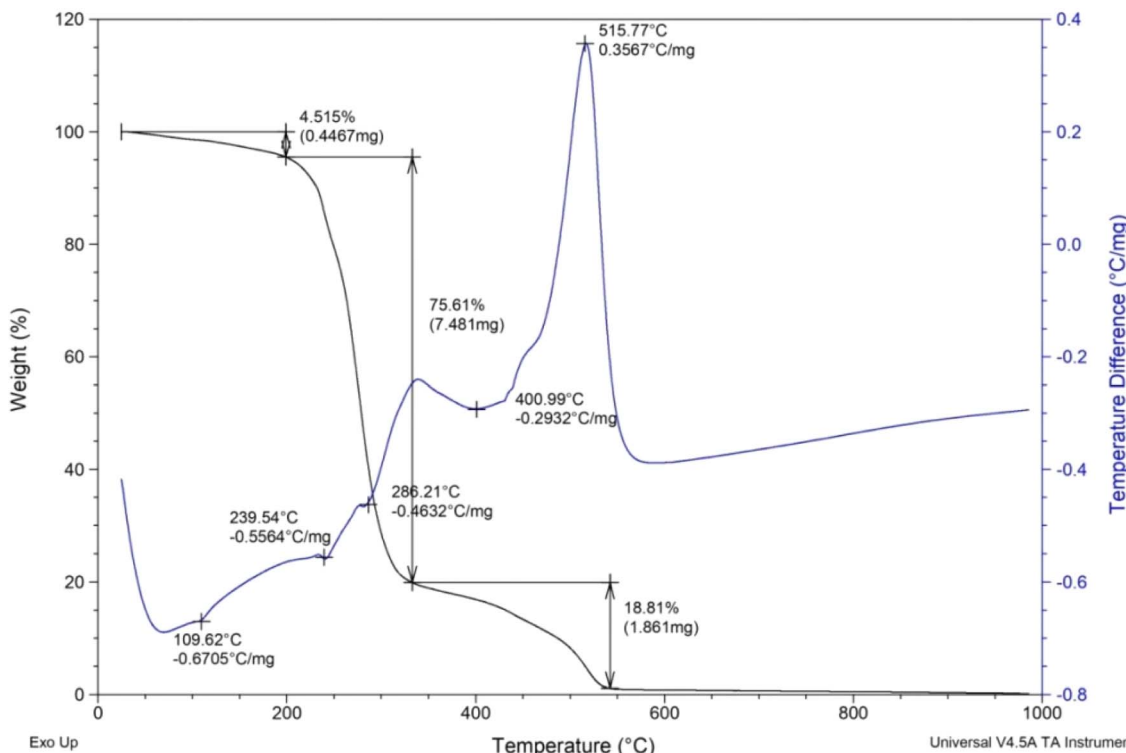


Fig. 4 TGA/DTA plot of  $[\text{HDMM}]^+ [\text{HSO}_4]^-$ .

minutes using line collimation. The sample-to-detector distance was 2500 millimeters. The detectors used were an Eiger R 1 M equipped with a vacuum lining and a high-resolution hybrid pixel photon counting system featuring a pixel size of 75  $\mu\text{m}$ . The sample was subjected to 15-minute exposure intervals, during which scattered waves were recorded across a momentum transfer range of  $q = 0.04$  to  $4 \text{ nm}^{-1}$  (eqn (1)):

$$q = \frac{4\pi \sin(\theta)}{\lambda}, \quad (1)$$

where  $\lambda$  = wavelength.

Fig. 5a and b show the intensity ( $I$ ) vs. scattering vector ( $q$ ) plots obtained from the scattering data of the SAXS measurements of  $[\text{HDMM}]^+ [\text{HSO}_4]^-$  surfactant micelle assembly in water. X-ray scattering was observed at  $q = 12.74 \text{ nm}^{-1}$ . The intermicellar separation distance ( $d_{\text{Bragg}}$ ) was determined to be 0.49 nm (eqn (2)):

$$d_{\text{Bragg}} = \frac{2\pi}{q_{\text{max}}}. \quad (2)$$

To determine the size of the spherical micelle system, the radius of gyration ( $R_G$ ) was calculated using Guinier's plot (Fig. 5c). Guinier's plot is obtained from the equation given below:

$$\ln[\Delta(q)] = \ln[a_0] - \frac{R_G^2 q^2}{3}, \quad (3)$$

where  $a_0$  is the zero angle intensity.

The radius of the gyration ( $R_G$ ) was 0.69 nm evaluated from the slope of  $\ln[\Delta(q)]$  vs.  $q^2$  plot. The straight line of the data points in the Guinier plot indicates the uniform size of the micelles formed in water. This confirms the introduction of a homogeneous distribution of equal-sized micelles. The average radius of the spherical particle ( $R$ ) was derived from the radius of gyration ( $R_G$ ) using the equation  $R = \sqrt{5/3R_G}$ . The average radius of the particle was detected to be 1.55 nm and the diameter is 3.1 nm. The average distance of separation was found to be 0.49 nm.<sup>44</sup>

## 2.2 Molecular geometry optimization

Ground state Density Functional Theory (DFT) calculation was performed on the surfactant molecule to optimize the geometrical structure. The DFT calculation was carried out at Becke's three-parameter functional and Lee-Yang-Parr hybrid functional (B3LYP) levels using the Gaussian 16 program. The 6-31G++(d,p) basis set was used for geometry optimization.<sup>45,46</sup> Calculations were performed in the gaseous phase. The optimized structure of the surfactant molecule is shown in Fig. 6. The optimized structure depicts weak hydrogen bonding of lengths 2.16 Å, 2.13 Å, and 1.98 Å existing between the oxygen of the anion and the hydrogen of the cation moiety. Hydrogen bonding is shown by dotted lines in Fig. 6. The Mulliken charge distribution of the optimized molecule calculated at the same level of calculation is shown in Fig. 7.

The highest occupied molecular orbital (HOMO) and lowest unoccupied molecular orbital (LUMO) of a surfactant molecule are shown in Fig. 8. HOMO is located on the non-bonding



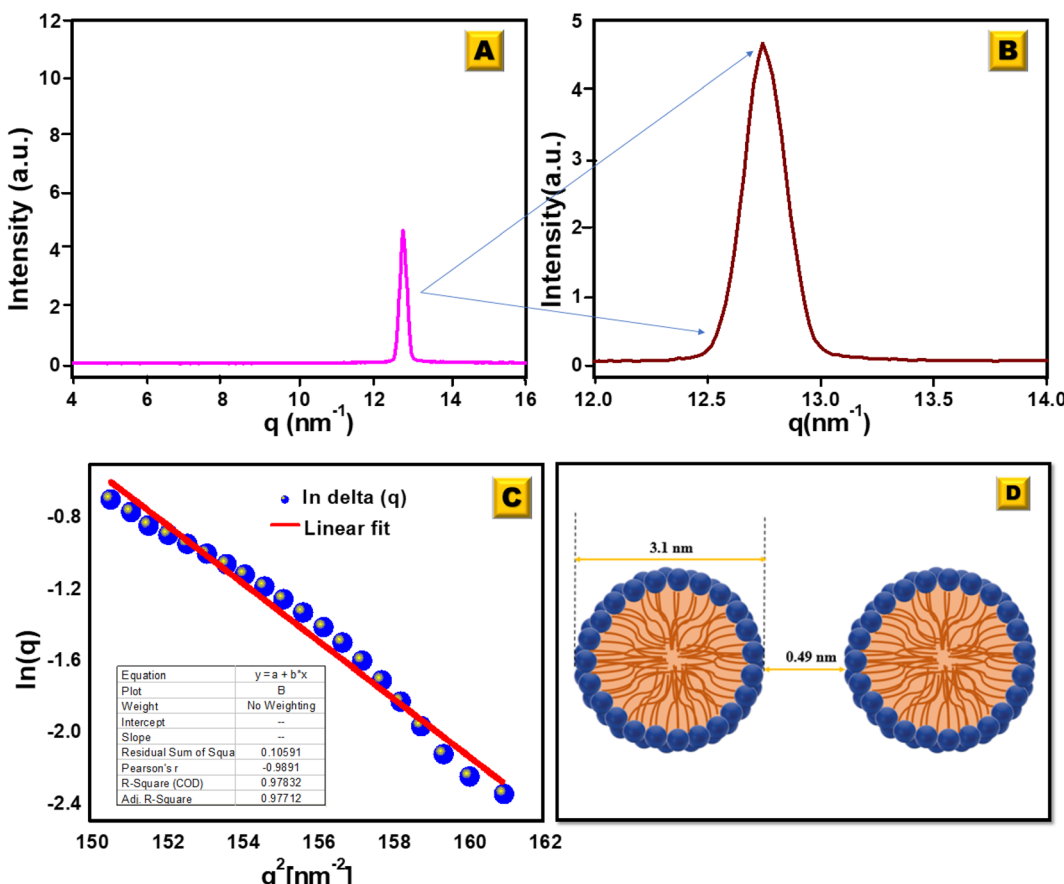


Fig. 5 (A) SAXS analysis for the  $[\text{HDMM}]^+ [\text{HSO}_4]^-$  surfactant in water. (B) Scattered peak position. (C) Guinier's plot. (D) Spacing between the micelle and diameter of the micelle.

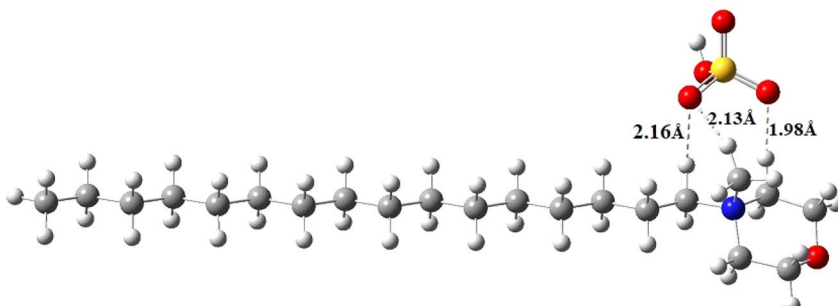


Fig. 6 Optimized structure of the surfactant molecule  $[\text{HDMM}]^+ [\text{HSO}_4]^-$ .

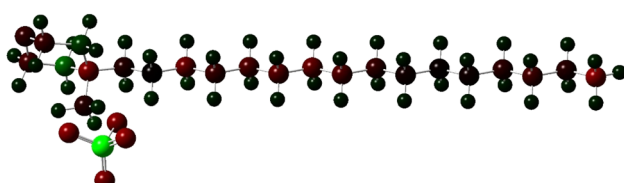


Fig. 7 Mulliken charge distribution on the surfactant molecule  $[\text{HDMM}]^+ [\text{HSO}_4]^-$  (the green color represents the positively charged atom, while the brown color represents the negatively charged atoms).

orbital of the oxygen atom of the anion moiety, while LUMO is localized mainly on the cyclohexane ring of the cation moiety.

### 2.3 Optimization study

After these major achievements, attention was turned towards exploring the catalytic efficiency of the synthesized catalyst,  $[\text{HDMM}]^+ [\text{HSO}_4]^-$ , to synthesize thiazolyl-pyrazole-chromen-2-one derivatives. The optimization of the catalyst was carried out using the model reaction of acetoacetyl coumarin, thiosemicarbazide and dimethyl acetylene dicarboxylate (DMAD) at room temperature. No significant yield was obtained for the



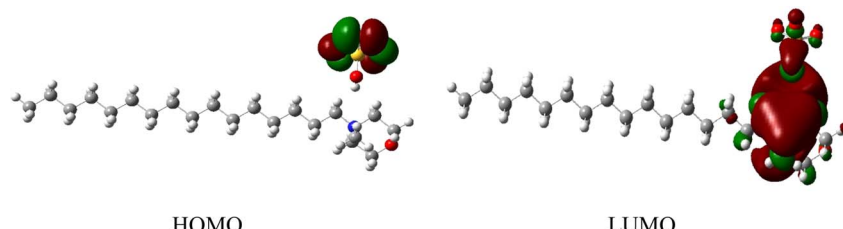


**Fig. 8** Frontier molecular orbital images of HOMO and LUMO of the surfactant molecule

reaction without a catalyst (Table 1, entry 1). Therefore,  $K_2CO_3$ ,  $NH_2-SO_3H$ , *p*-TSA,  $\gamma$ -proline, cetyltrimethyl ammonium bromide (CTAB), sodium dodecyl sulphate (SDS), Triton X-100, sodium dioctyl sulfosuccinate (SDOSS), benzethonium chloride

**Table 1** Screening of catalysts for the formation of thiazolyl-pyrazole-chromen-2-ones (**4a**)<sup>a</sup>

Entry	Catalyst	Catalyst load (mol%)	Time (h)	Yield <sup>b</sup> (%)
1	—	—	12–24	20
2	K <sub>2</sub> CO <sub>3</sub>	20	20	40
3	NH <sub>2</sub> –SO <sub>3</sub> H	20	6.2	78
4	<i>p</i> -TSA	20	5	80
5	L-Proline	20	7	70
6	CTAB	20	18	55
7	SDS	15	24	58
8	Triton X 100	20	24	61
9	SDOSS	20	20	48
10	[BZT] <sup>+</sup> Cl <sup>−</sup>	20	11	55
11	[BZT] <sup>+</sup> AlCl <sub>4</sub> <sup>−</sup>	20	6	75
12	[HDMMM] <sup>+</sup> HSO <sub>4</sub> <sup>−</sup>	10	4	80
13	[HDMMM] <sup>+</sup> HSO <sub>4</sub> <sup>−</sup>	15	3	83
14	[HDMMM] <sup>+</sup> HSO <sub>4</sub> <sup>−</sup>	20	2.5	89
15	[HDMMM] <sup>+</sup> HSO <sub>4</sub> <sup>−</sup>	25	3	90

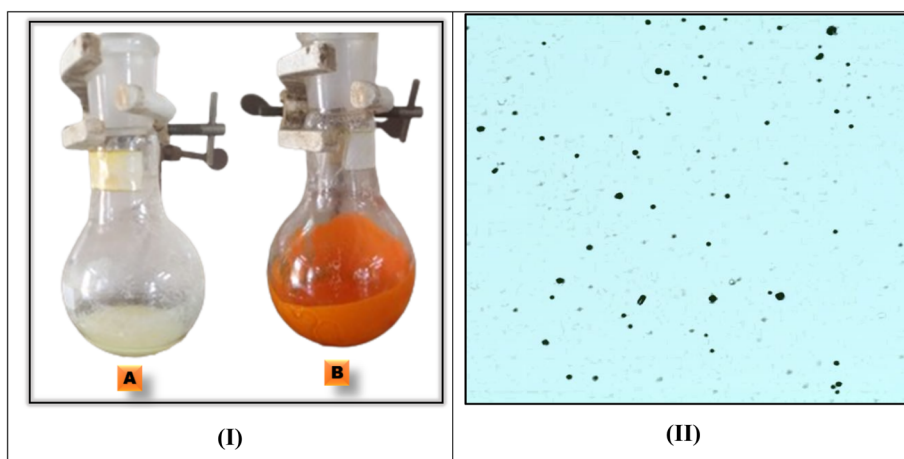
<sup>a</sup> Reaction conditions: acetoacetyl coumarin (1 mmol), thiosemicarbazide (1 mmol), dialkyl acetylene dicarboxylate (1 mmol), specific catalyst, water (5 mL), RT. <sup>b</sup> Isolated yield.

$[\text{BZT}]^+$   $\text{Cl}^-$ ,  $[\text{BZT}]^+$   $\text{AlCl}_4^-$  and  $[\text{HDMM}]^+$   $[\text{HSO}_4]^-$  are screened for model reaction (Table 1, entries 2–12).

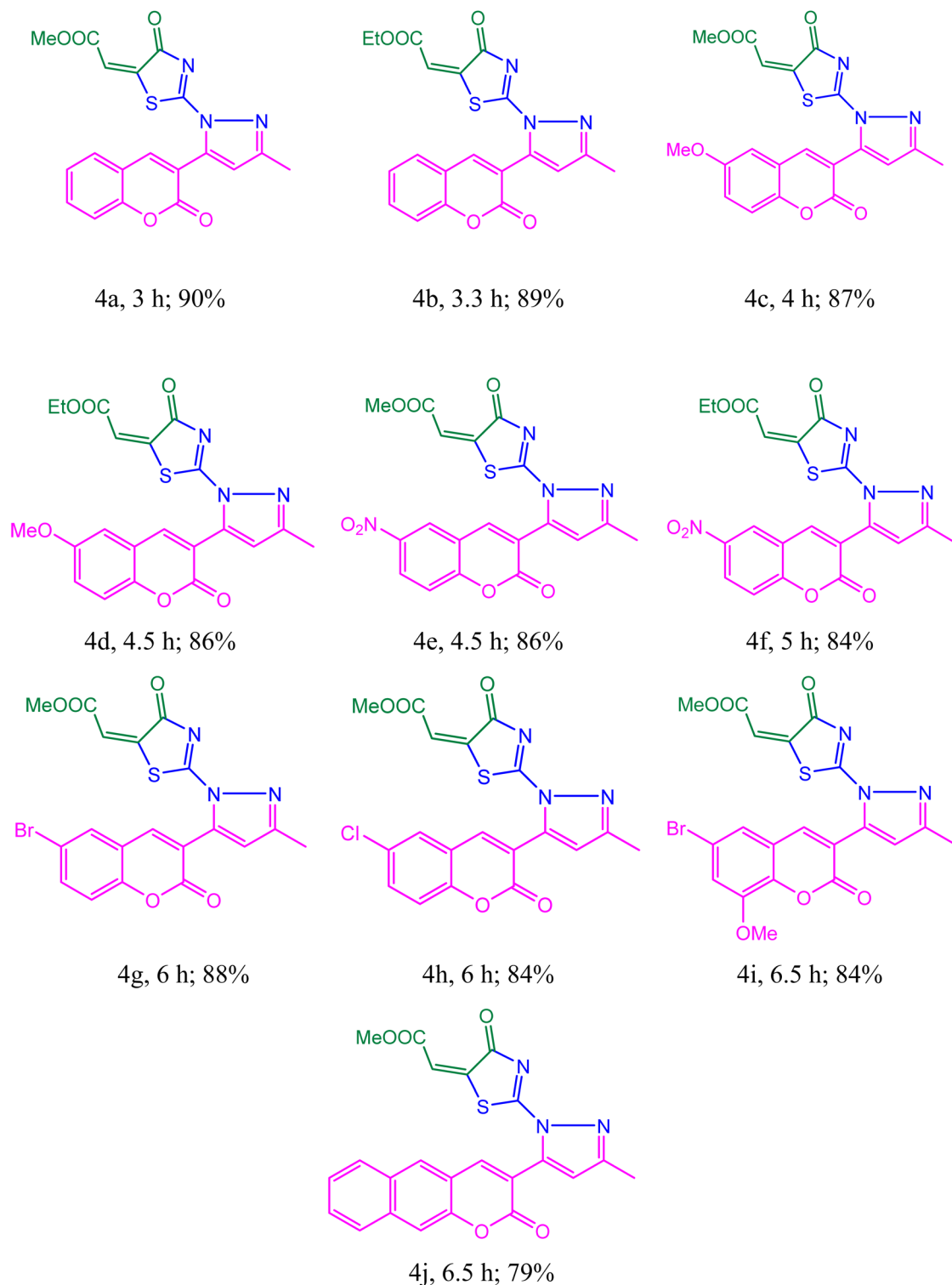
$\text{K}_2\text{CO}_3$  as a catalyst provides a low yield of the desired product (Table 1, entry 2). The yield was sufficiently increased for the reactions in the acid catalysts (Table 1, entries 3–5, and 11). Commercially available surfactants, *viz* cetyltrimethyl ammonium bromide (CTAB), sodium dodecyl sulfate (SDS), Triton X-100, sodium dioctyl sulfosuccinate (SDOSS) and benzethonium chloride  $[\text{BZT}]^+ \text{Cl}^-$ , gave moderate yield in aqueous medium (Table 1, entries 6–10). Pleasingly,  $[\text{HDMM}]^+ [\text{HSO}_4]^-$  exhibited a high yield (Table 1, entry 14). Thus, amongst the catalysts screened,  $[\text{HDMM}]^+ [\text{HSO}_4]^-$  was found to be superior for performing the reaction at room temperature.

The effect of catalyst loading was also studied for the model reaction. The 20 mol% of  $[\text{HDMM}]^+ [\text{HSO}_4]^-$  was found to be tolerable in promoting this reaction (Table 1, entries 12–15). Catalyst loading greater than 20% did not positively influence both the yield and reaction time.

The reaction mixture of acetoacetylcoumarin and thiocarbazide was converted into a homogeneous solution by adding a surfactant. The formation of white turbid emulsion confirms the formation of micelles or colloidal aggregates [Fig. 9(I)]. Finally, an orange precipitate was obtained after the addition of DMAD, indicating the completion of the reaction. The formation of spherical emulsion droplets (microbubbles) in the aqueous medium was confirmed by taking an optical microscopic image [Fig. 9(II)].



**Fig. 9** (I) (A) Reaction mixture at intermediate (acetoacetylcoumarine + thiosemicarbazide). (B) Reaction mixture after the completion of the reaction (after the addition of DMAD). (II) Optical micrograph image of the reaction mixture in water.

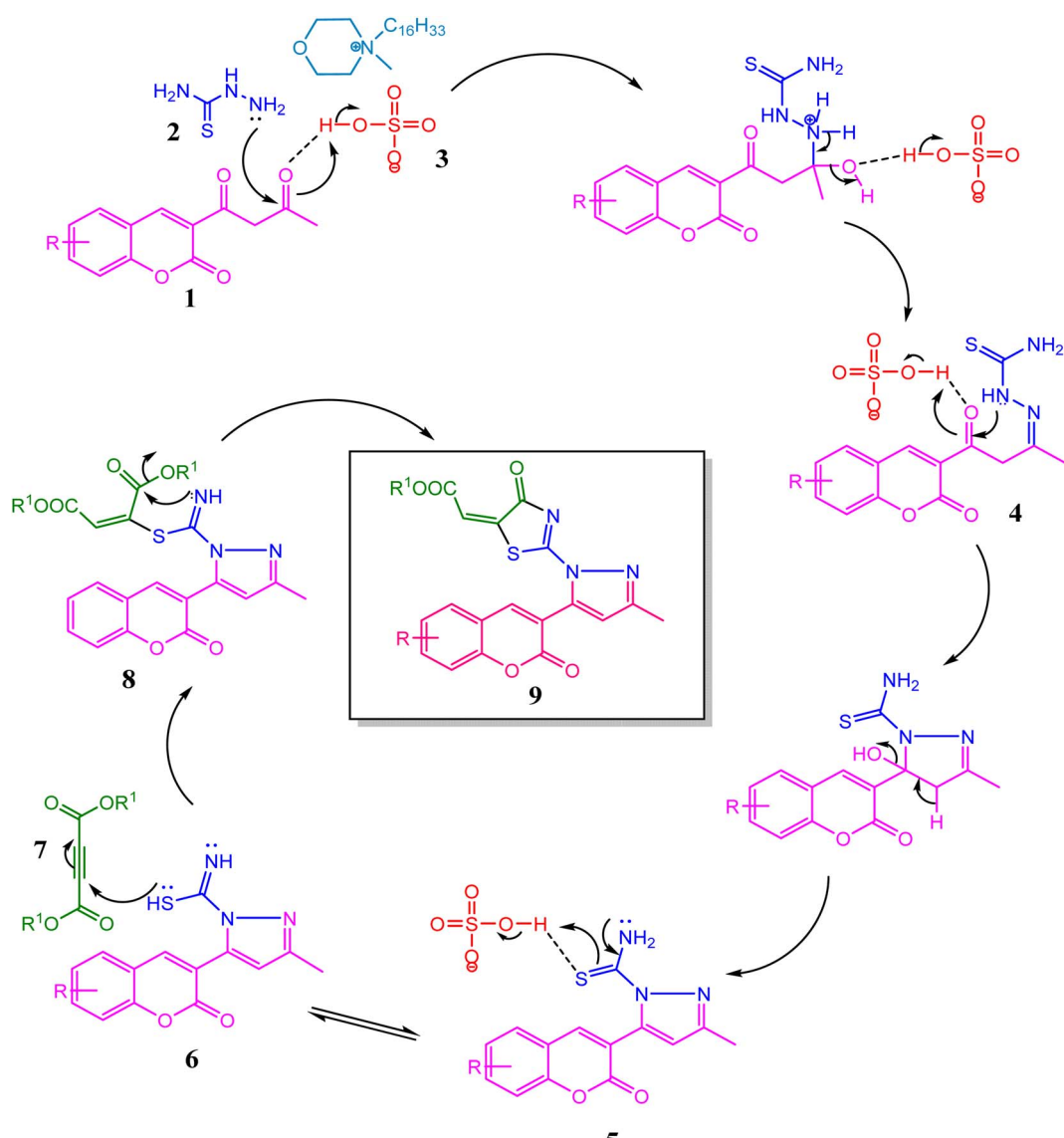
Table 2 Synthesis of a combinatorial library of thiazolyl-pyrazole-chromen-2-one derivatives<sup>a</sup>

<sup>a</sup> Reaction conditions: acetoacetylcoumarin (1 mmol), thiosemicarbazide (1 mmol), dialkyl acetylene dicarboxylate (1 mmol), catalyst:  $[\text{HDMM}]^+$   $[\text{HSO}_4]^-$  (20%), water (5 mL), room temperature.

Notably, the workup of the reaction was carried out by simple filtration and recrystallization in hot ethanol to produce an extremely pure product. Based on spectral information, the

structure of the product was confirmed (**4a**). Infrared analysis of compound **4a** exhibited absorption bands at 1719, 1687 and 1347  $\text{cm}^{-1}$  due to lactone ( $\text{C}=\text{O}$ ), imine ( $\text{C}=\text{N}$ ), and ( $\text{C}-\text{S}$ )





Scheme 3 Plausible reaction mechanism for the synthesis of thiazolyl-pyrazole-chromen-2-ones.

stretching frequencies, respectively. The <sup>1</sup>H NMR and <sup>13</sup>C NMR spectra of **4a** concluded that the product was isometrically pure. The <sup>1</sup>H NMR study of methyl (*E*)-2-(2-(3-methyl-5-(2-oxo-2*H*-chromen-3-yl)-1*H*-pyrazol-1-yl)-4-oxothiazol-5(4*H*)ylidene)acetate **4a** showed that the singlet of vinylic proton at  $\delta$  = 6.73 ppm clearly indicates the *E*-configuration of the exocyclic double bond of the thiazolidinone ring.<sup>47-49</sup> The presence of vinylic proton above 6.90 ppm supported the *Z*-configuration.<sup>50</sup> The peaks at  $\delta$  2.34 ppm and 3.87 ppm are due to methyl and methoxy protons, respectively. The singlet corresponding to the methine proton of pyrazole and coumarin is observed at  $\delta$  6.69 and 8.41 ppm, respectively. The aromatic protons of the coumarin skeleton were observed at  $\delta$  7.37–8.02 ppm. <sup>13</sup>C NMR analysis also confirmed the structural identity, with resonance observed at  $\delta$  15.89 (–CH<sub>3</sub>), 52.06 (–OMe), 100.42 (pyrazol–CH), 114.81, 116.15, 118.59, 118.77, 124.82, 126.10, 129.20 (coumarin Ar–CH), 129.79, 132.29, 140.71 (pyrazole C–N), 141.77 (pyrazole

C=N), 142.72, 146.05 (coumarin –CH), 153.06 (=CH–COOMe), 153.24 C=C thiazole), 161.09 (C=N thiazole), 163.91 (–CO lactone), 166.12 (–CO ester) and 170.89 (–CO–amide). The

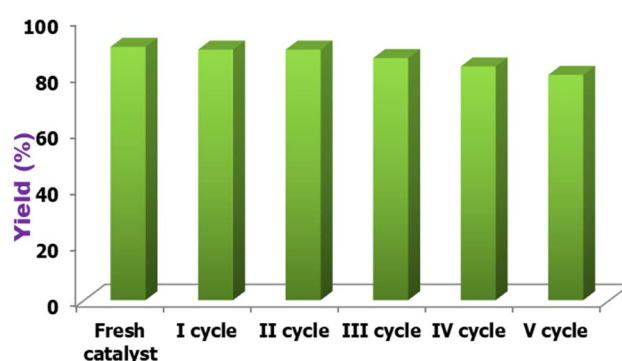


Fig. 10 Recyclability study of [HDMM]<sup>+</sup> [HSO<sub>4</sub>]<sup>-</sup>.



molecular ion peak of compound **4a** was found in the mass spectrum at  $m/z = 395.39$   $[M]^+$ , corresponding to the molecular formula  $C_{19}H_{13}N_3O_5S$ . All the above spectroscopic data clearly indicate the formation of the target product.

With improved reaction conditions in hand, we expanded the scope of the reaction using various structurally diverse acetoacetyl coumarin derivatives with dimethyl and diethyl acetylene dicarboxylates (DMAD and DEAD) [Table 2]. Interestingly, acetoacetyl coumarin with electron-withdrawing and electron-donating substituents was almost inevitably transformed into its respective targets with an excellent yield (Table 2, product **4c–4i**).

Eventually, the competency of the reaction was examined using an acetoacetyl coumarin derivative synthesized from 2-hydroxy naphthaldehyde, and it was found that the reaction performed well with a good yield (Table 2, product **4j**).

A plausible mechanism for the formation of thiazolyl-pyrazole-chromen-2-ones is depicted in Scheme 3. Initially, the condensation of thiosemicarbazide **2** with acetoacetyl coumarin **1** results in the formation of Knorr-pyrazole skeleton **5**. The sulphur atom of **6** as thiol after prototropic tautomeric shift attacks one of the ethynyl carbons of DMAD **7** in a Michael addition manner to yield *S*-alkylated intermediate **8**, followed by an intramolecular amidation reaction to yield product **9**. Overall, the reaction generates one C–S, one C=N, and two C–N bonds. Simultaneously, thiazole and pyrazole heterocycles were developed successively.

Because catalyst reusability is an essential economic consideration, recovery and reusability experiments were conducted for the reaction of acetoacetyl coumarin, thiosemicarbazide, and dimethyl acetylene dicarboxylate. Following the reaction, the product was filtered and washed multiple times with 25 mL of water. The collected filtrate was concentrated on a rotary evaporator to 5 mL, and the filtrate remaining in the flask was washed with diethyl ether before being reused immediately by adding substrates in the next cycle, with no additional purification. As shown in Fig. 10, the catalyst can be reused five times without a significant decrease in catalytic activity.

### 3 Conclusion

In conclusion, we developed a new, facile, one-pot multi-component synthesis of substituted thiazolyl-pyrazole-chromen-2-ones from acetoacetyl coumarin, thiosemicarbazide, and dialkyl acetylene dicarboxylate in the presence of  $[HDMM]^+ [HSO_4]^-$  as an effective Brønsted acidic surfactant. The small angle X-ray scattering (SAXS) analysis and ground state Density Functional Theory (DFT) calculation confirmed the size and geometrical structure of the surfactant molecule. This approach provides various advantages, such as the use of water as a universal solvent, short reaction time, good yields, wide substrate scope, easy work-up, and furnishing a pure product without tedious column chromatography. This transformation established the formation of four bonds: one C–S, one C=N, and two C–N bonds. It also generated thiazole and

pyrazole heterocycles. The synthesized derivatives containing three heterocyclic rings may be beneficial in drug discovery.

### Data availability

The data supporting this article have been included as part of the ESI.<sup>†</sup>

### Author contributions

Mayuri Patil: conceptualization, methodology, writing – original draft preparation. Pradeep Mhaldar: methodology, software, data curation, Vrushali Mahadik: visualization, writing – reviewing and editing Rinku Ghanta and Madhulata Shukla: software, validation. Suraj Sonawane: writing – reviewing and editing Suresh K. Ghote kar: visualization, writing – reviewing and editing Gajanan Rashinkar: supervision, writing original draft Dattaprasad Pore: supervision, visualization, writing – reviewing and editing.

### Conflicts of interest

There are no conflicts to declare.

### Acknowledgements

MVP is thankful to Shivaji University, Kolhapur for providing Golden Jubilee Research Fellowship (Ref. No. SU/CUDC/UGK/GJRF/16/2019-20/763) of the Department of Industrial Chemistry.

### References

- 1 (a) R. T. Baker and W. Tumas, *Science*, 1999, **284**, 1477; (b) P. T. Anastas and J. C. Warner; *Green Chemistry: Theory and Practice*, Oxford University Press, Oxford, 1998; (c) J. Haggan, *Chem. Eng. News*, 1994, **72**, 22; (d) E. M. Kirschner, *Chem. Eng. News*, 1994, **72**, 13; (e) D. L. Illman, *Chem. Eng. News*, 1994, **72**, 22.
- 2 N. Azizi, A. K. Amiri, R. Baghi, M. Bolourchian and M. M. Hashemi, *Monatsh. Chem.*, 2009, **140**, 1471.
- 3 P. A. Grieco, *Organic Synthesis in Water*, Blackie Academic and Professional, 1998.
- 4 C. J. Li, *Chem. Rev.*, 1993, **93**, 2023.
- 5 C. J. Li, *Chem. Rev.*, 2005, **105**, 3095.
- 6 C. J. Li and T. H. Chan, *Organic Reaction in Aqueous Media*, Wiley New York, 1997.
- 7 M. C. Pirrung and K. D. Sarma, *J. Am. Chem. Soc.*, 2004, **126**, 444.
- 8 A. Shaabani, A. Rahmati, A. H. Rezayan, M. Darvishi, Z. Badri and A. Sarvari, *QSAR Comb. Sci.*, 2007, **26**, 973.
- 9 W. Wei, C. C. K. Keh, C. J. Li and R. S. Varma, *Environ. Sci. Policy*, 2004, **6**, 250.
- 10 A. Chanda and V. V. Fokin, *Chem. Rev.*, 2009, **109**, 725.
- 11 H. Zhou, S. Wu, S. Zhai, A. Liu, Y. Sun, R. Li, Y. Zhang, S. Ekins, P. W. Swaan, B. Fang, B. Zhang and B. Yan, *J. Med. Chem.*, 2008, **51**, 1242.



12 M. G. Vigorita, R. Ottana, F. Monforte, R. Maccari, M. T. Monforte, A. Trovato, M. F. Taviano, N. Miceli, G. D. Luca, S. Alcaro and F. Ortuso, *Bioorg. Med. Chem.*, 2003, **11**, 999.

13 S. Bondock, W. Khalifa and A. A. Fadda, *Eur. J. Med. Chem.*, 2007, **42**, 948.

14 S. V. K. Archana and A. Kumar, *Indian J. Pharm. Sci.*, 2003, **65**, 358.

15 K. Omar, A. Geronikaki, P. Zoumpoulakis, C. Camoutsis, M. Sokovic, A. Ceric and J. Glamocilja, *Bioorg. Med. Chem.*, 2010, **18**, 426.

16 K. Babaoglu, M. A. Page, V. C. Jones, M. R. McNeil, C. Dong, J. H. Naismithc and R. E. Lee, *Bioorg. Med. Chem. Lett.*, 2003, **13**, 3227.

17 H. Chen, T. Yang, S. Wei, H. Zhang, R. Li, Z. Qin and X. Li, *Bioorg. Med. Chem. Lett.*, 2012, **22**, 7041.

18 G. C. Look, J. R. Schullek, C. P. Holmes, J. P. Chinn, E. M. Gordon and M. A. Gallop, *Bioorg. Med. Chem. Lett.*, 1996, **6**, 707.

19 F. A. R. Ruiz, R. N. Garcia-Sanchez, S. V. Estupinan, A. Gomez-Barrio, D. F. T. Amado, B. M. Perez-Solorzano, J. J. Nogal-Ruiz, A. R. Martinez- Fernandez and V. V. Kouznetsov, *Bioorg. Med. Chem.*, 2011, **19**, 4562.

20 H. Chen, L. Hao, M. Zhu, T. Yang, S. Wei, Z. Qin, P. Zhang and X. Li, *Bioorg. Med. Chem. Lett.*, 2014, **24**, 3426.

21 A. Zarghi, T. Zebardast, B. Daraie and M. Hedayati, *Bioorg. Med. Chem.*, 2009, **17**, 5369.

22 N. Rahuja, A. Mishra, S. Gautam, A. K. Tamrakar, R. Maurya, S. K. Jain and A. K. Srivastava, *Int. J. Pharm. Sci. Rev. Res.*, 2013, **22**, 121.

23 S. Raza, S. P. Srivastava, D. S. Srivastava, A. K. Srivastava, W. Haq and S. B. Katti, *Eur. J. Med. Chem.*, 2013, **63**, 611.

24 R. Perez-Fernandez, P. Goya and J. Elguero, *ARKIVOC*, 2014, 233.

25 P. D. Sauzem, P. Machado, M. A. Rubin, G. Da, S. Sant Anna, H. B. Faber, A. H. De Souza, C. F. Mello, P. Beck, R. A. Burrow, H. G. Bonacorso, N. Zanatta, M. A. P. Martins and D. Patricia, *Eur. J. Med. Chem.*, 2008, **43**, 1237.

26 M. N. A. Nasr and S. A. Said, *Arch. Pharm.*, 2003, **336**, 551.

27 G. Turan-Zitouni, P. Chevallet, F. S. Killic and K. Erol, *Eur. J. Med. Chem.*, 2000, **35**, 635.

28 Z. A. Kaplancikli, G. Turan-Zitouni, A. Ozdemir, G. Revial and K. Guven, *Phosphorus, Sulfur Silicon Relat. Elem.*, 2007, **182**, 749.

29 R. B. Pathak and S. C. Bahel, *J. Indian Chem. Soc.*, 1980, **57**, 1108.

30 N. Shankaraiah, V. Devaiah, K. L. Reddy, A. Juvekar, S. Sen, N. Kurian and S. Zingde, *Bioorg. Med. Chem. Lett.*, 2008, **18**, 1468.

31 S. Lee and S. B. Park, *Org. Lett.*, 2009, **11**, 5214.

32 J. Orrego-Hernandez, J. Cobo and J. Portilla, *Eur. J. Org. Chem.*, 2015, **23**, 5064.

33 M. Moreno-Manas and R. Pleixats, *Advances in Heterocyclic Chemistry*, Academic Press, San Diego, CA, 1996, vol. 53, p. 1.

34 D. Egan, E. O Kennedy, E. Moran, D. Cox, E. Prosser and R. D. Thornes, *Drug Metab. Rev.*, 1990, **22**, 503.

35 (a) C. Kontogiorgis and D. Hadjipavlou-Litina, *J. Enzyme Inhib. Med. Chem.*, 2003, **18**, 63; (b) C. Spino, M. Dodier and S. Sotheeswaran, *Bioorg. Med. Chem. Lett.*, 1998, **8**, 3475; (c) I. Kempen, D. Papapostolou, N. Thierry, L. Pochet, S. Counerotte, B. Masereel, J. M. Foidart, M. J. Reboud-Ravaux, A. Noel and B. Pirotte, *Br. J. Cancer*, 2003, **88**, 1111; (d) S. Vilar, E. Quezada, L. Santana, E. Uriarte, M. Yanez, N. Fraiz, C. Alcaide, E. Cano and F. Orallo, *Bioorg. Med. Chem. Lett.*, 2006, **16**, 257; (e) E. Quezada, G. Delogu, C. Picciau, L. Santana, G. Podda, F. Borges, V. Garcia-Moraes, D. Vina and F. Orallo, *Molecules*, 2010, **15**, 270.

36 Y. Wang, B. Li, S. Liu, Z. Wen, J. Yang, H. Zhang and X. Hao, *J. Nat. Prod.*, 2017, **80**, 798.

37 Y. Ma, C. Zhang, W. Zhao, S. Shi, D. He, P. Zhang, X. Liu, T. Han, Y. Fu and Y. Liu, *Nat. Prod. Res.*, 2018, **32**, 2159.

38 D. A. Horton, G. T. Bourne and M. L. Smythe, *Chem. Rev.*, 2003, **103**, 893.

39 H. Kohjiro, S. Kazuhiro, O. Yasuyo, S. Akira, S. Sadaharu and A. Hironori, *Chem. Commun.*, 2001, **6**, 569.

40 G. He, X. Zhang, C. He, X. Zhao and C. Duan, *Tetrahedron*, 2010, **66**, 9762.

41 (a) J. M. Lang and H. G. Drickamer, *J. Phys. Chem.*, 1993, **97**, 5058; (b) A. R. A. Palmans, P. Smith and C. Weder, *Macromolecules*, 1999, **32**, 4677.

42 (a) M. A. Tlenkopatchev, S. Fomine, L. Fomina, R. Gavino and T. Ogawa, *Polym. J.*, 1997, **29**, 622; (b) S. Fomine, C. Delgado, L. Fomina, R. Gavino and T. Ogawa, *Macromol. Chem. Phys.*, 1997, **198**, 3065; (c) S. Fomine, L. Fomina, C. Sanchez, A. Ortiz and T. Ogawa, *Polym. J.*, 1997, **29**, 49; (d) S. Fomine, H. Perez, L. Fomina, M. Tlenkopatchev and T. Ogawa, *Macromol. Chem. Phys.*, 1997, **198**, 1679; (e) S. Fomine, E. Rivera, L. Fomina, A. Ortiz and T. Ogawa, *Polymer*, 1998, **39**, 3551.

43 O. R. Gottlieb, K. Herrmann, R. D. H. Murray, G. Ohloff and G. Pattenden, *fortschr. Chem. Org. Naturst.*, 2012, 35.

44 M. V. Patil, P. M. Mhaldar, S. N. Tayade, G. S. Rashinkar and D. M. Pore, *J. Mol. Liq.*, 2022, **359**, 119305.

45 A. D. Becke, *J. Chem. Phys.*, 1993, **98**, 5648.

46 C. Lee, W. Yang and R. G. Parr, *Phys. Rev. B: Condens. Matter Mater. Phys.*, 1988, **37**, 785.

47 V. A. Bakulev, V. S. Berseneva, N. P. Belskaia, Y. Y. Morzherin, A. Zaitsev, W. Dehaen, I. Luyten and S. Toppet, *Org. Biomol. Chem.*, 2003, **1**, 134.

48 M. S. Mirakmahaleh, K. Rad-Moghadam, H. Kefayati and S. Falakro, *Mol. Diversity*, 2020, **25**, 109.

49 Z. Ahani, M. Nikbin, M. Maghsoodlou, F. Farhadi-Ghalati, J. Valizadeh, H. Beyzaei and M. Moghaddam-Manesh, *J. Iran. Chem. Soc.*, 2018, **15**, 2423.

50 A. A. Hassan, A. A. Aly, M. Ramadan, N. K. Mohamed, H. N. Tawfeek and M. Nieger, *Monatsh. Chem.*, 2020, **151**, 1453.

